The Phase $Co_{1-x}Ni_xSn_2$: Structural Variations Based on the Stacking of Two Different Planar Nets

Ulrich Häussermann,* Angel R. Landa-Cánovas,† and Sven Lidin

Department of Inorganic Chemistry 2, Lund University, P.O. Box 124, S-22100 Lund, Sweden

Received March 18, 1997[⊗]

The investigation of the tin-rich part of the ternary system Co/Ni/Sn yielded the phase $Co_{1-x}Ni_xSn_2$ with the range of composition $0.23(3) < x < 0.59(3)$. When using a large excess of tin, $Co_{1-x}Ni_xSn_2$ crystallizes at 500 °C in a structure isotypic to that of tetragonal $PdSn_2$ whereas a modification with the orthorhombic $CoGe_2$ structure type always forms from a stoichiometric mixture of the elemental components or from a tin melt at temperatures above 550 °C. The structures of $Co_{0.625}Ni_{0.375}Sn_2$ were determined by single-crystal X-ray diffraction methods ($PdSn_2$-type space group $I4_1/acd$, $a = 6.2360(5)$ Å, $c = 23.588(2)$ Å, $Z = 16$; $CoGe_2$-type space group $Aba2$, $a = 6.2439(4)$ Å, $b = 6.2493(4)$ Å, $c = 11.778(1)$ Å, $Z = 8$). Both structures have the same building unit consisting of three consecutive planar nets 4^4, 3^2434, 4^4 formed by tin atoms. The condensation of the building blocks in the c direction gives rise to different stacking sequences. In the $PdSn_2$-type, a ABCD sequence is realized and the c axis is doubled compared to the ideal $CoGe_2$-type with AB stacking. Electron diffraction and high-resolution electron microscopy studies revealed the existence of other, complex, stacking variants as well as stacking faults in the $Co_{1-x}Ni_xSn_2$ system.

Introduction

Frequently, the chemical description of structural stability of binary intermetallic compounds is made in terms of the difference in electronegativity and size of the constituting atoms and the number of electrons per atom or per formula unit.[1] If this so-called valence electron concentration (VEC) mainly controls the stability of a crystal structure, the phases concerned are classified as electron compounds and the Hume−Rothery phases may serve as classical examples.[2,3]

During our investigation of the importance of VEC on the structural stability of compounds T_mE_n with T a transtion metal and E an E13 or E14 element (i.e., Al, Ga, Sn), we found a fascinating series of VEC-induced phase transitions in the quasibinary systems $T_{1-x}T'_xSn_2$ (T, T′ = Ti, V, Cr, Fe, Co, Ni) (Figure 1). The distannides of V and Cr crystallize in the $CuMg_2$ structure type and those of Mn, Fe, and Co in the $CuAl_2$-type, whereas the compounds $TiSn_2$ and $NiSn_2$ do not exist. In the quasibinary systems, three more structure types occur. The hitherto rare $NiMg_2$-type was found in several of these systems when the VEC is in the range between 14 ($CrSn_2$) and 15 ($MnSn_2$) electrons per formula unit. Thus, with increasing VEC, the sequence $CuMg_2 \rightarrow NiMg_2 \rightarrow CuAl_2$ of closely related structures is obtained.[4,5] At still higher values of VEC, as realized in the $Co_{1-x}Ni_xSn_2$ system, the structure types $PdSn_2$ and $CoGe_2$ appear.

In this article, we report on the synthesis of this new phase $Co_{1-x}Ni_xSn_2$ and the crystal structures of its low- and high-temperature modifications. The structures contain as an important motif the planar 3^2434 net formed by Sn atoms (Figure 2). This net has square symmetry and can be obtained from the square 4^4 net by simply shearing half of the squares to diamonds.[6] It occurs frequently in the structures of T_mE_n compounds where it is formed by the E atoms.[6,7] An important feature of the 3^2434 net is the possibility of stacking it differently, and for example, the crystal structures of the $Co_{1-x}Ni_xSn_2$ modifications are distinguished by a different

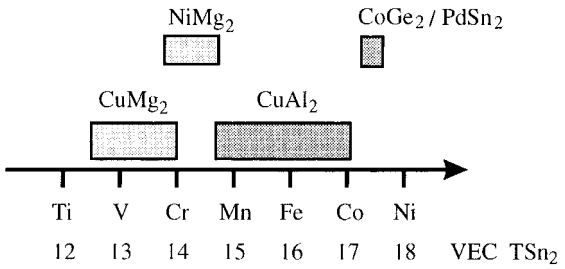

Figure 1. Relationship between the valence electron concentration (VEC; number of electrons per formula unit) and the observed crystal structures in the systems $T_{1-x}T'_xSn_2$.

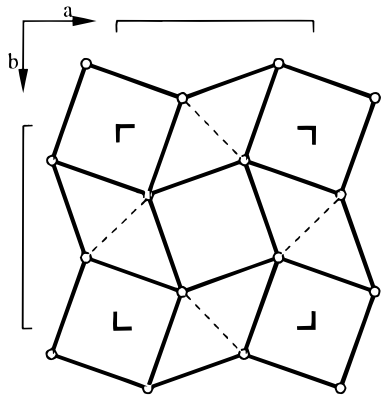

Figure 2. The square 3^2434 net consisting of diamonds and squares.

† Centro de Microscopia Electronica 'Luis Bru', Universidad Complutense de Madrid, ES-28040 Madrid, Spain

⊗ Abstract published in *Advance ACS Abstracts,* August 1, 1997.

(1) Villars, P.; Mathis K.; Hulliger, F. In *The Structure of Binary Compounds*; de Boer, F. R. Pettifor, D. G., Eds.; Elsevier: New York, 1989; Chapter 1.
(2) Ferro, R.; Saccone, A. In *The Structure of Solids*; Cahn, R. W., Haasen, P., Kramer, E. J., Eds.; VCH: Weinheim 1993; Vol. 1, Chapter 3.
(3) Hoistad, L. M.; Lee, S. *J. Am. Chem. Soc.* **1991**, *113*, 8216.
(4) Larsson A.-K.; Lidin, S. *J. Alloys Compd.* **1995**, *221*, 136.
(5) Häussermann, U.; Lidin, S. Manuscript in preparation.
(6) Hyde, B. G.; Andersson, S. *Inorganic Crystal Structures*; John Wiley & Sons: New York, 1989.
(7) Pearson, W. B. *The Crystal Chemistry and Physics of Metals and Alloys*; John Wiley & Sons: New York, 1972.

S0020-1669(97)00313-3 CCC: $14.00

stacking sequence of this net. Different stacking possibilities might also increase the propensity of one-dimensional (stacking) disorder in such systems. We observed indeed, depending on the synthesis conditions, a complex situation of stacking disorder in $Co_{1-x}Ni_xSn_2$ crystals ranging from ordinary microscopic domain twinning to incommensurate stacking sequences.

Experimental Section

Synthesis. In order to study the quasibinary system $Co_{1-x}Ni_xSn_2$, we prepared samples from a mixture of the pure elements (Co powder, 99.5%, Kebo; Ni powder, puriss., Fluka; Sn powder, 99.5%, Aldrich) containing a total amount of 1 mmol of transition metal with the following compositions $x = 0.125, 0.25, 0.375, ..., 0.875$ (samples A, B, C, ..., G). The binary compound $CoSn_2$ ($x = 0$) crystallizes in the $CuAl_2$ structure, while a compound $NiSn_2$ ($x = 1$) is not known. In the Ni/Sn system, Ni_3Sn_4 is the compound with the highest Sn content.[8] Syntheses were performed in two different ways. In one series we used a stoichiometric amount of Sn (2 mmol), and in the other we added a large excess of Sn (10 mmol), thus using it as reactant and flux medium. The carefully mixed reactants were pressed to pellets and loaded into quartz ampules which were sealed under vacuum. Samples were heated at either 500, 550, or 900 °C for 3 days and then cooled to room temparature at an approximate rate of 100 °C/h. Excess Sn was dissolved with 4 M HCl. The samples were characterized by Guinier powder diagrams (Cu Kα; Si standard) and their composition analyzed with the EDX (energy-disperse X-ray) method in a JEOL scanning electron microscope averaging between 5 and 10 analyses for each sample.

In case of the stoichiometric mixture syntheses, the product from sample A was a mixture of $Co_{1-x}Ni_xSn_2$ in the $CuAl_2$ ($x \approx 0.05$) and the $CoGe_2$ structure. Samples B−D only exhibited $Co_{1-x}Ni_xSn_2$ in the $CoGe_2$ structure. In sample E, the phase $Ni_{3-x}Co_xSn_4$ (Ni_3Sn_4 structure) appeared and became the main product in the samples with even higher Ni contents. When applying synthesis temperatures of 500 and 550 °C, the product was a fine powder of grey color without suitable single crystals for an X-ray structure determination, whereas samples which had been heated at 900 °C were highly crystalline. X-ray powder patterns of samples with the same composition but different synthesis temperatures were found to be identical. When performing flux syntheses, reaction temperature plays a crucial role. With a temperature of 500 °C, the product of sample A was a mixture of $Co_{1-x}Ni_xSn_3$[9] and $Co_{1-x}Ni_xSn_2$ in the $PdSn_2$ structure. In samples B−D, $Co_{1-x}Ni_xSn_2$ in the $PdSn_2$ structure was found as the only product, and again the phase $Ni_{3-x}Co_xSn_4$ appeared in samples with higher Ni contents. When the synthesis temperature was raised to 550 °C, $Co_{1-x}Ni_xSn_2$ crystallizes in the $CoGe_2$ and not in the $PdSn_2$ structure. Crystals obtained from the flux synthesis were larger (sometimes several millimeters) compared to those obtained from a stoichiometric mixture synthesis. Single crystals exhibited a metallic luster with the habits of tetragonal rods ($PdSn_2$ structure) and thin rectangular plates ($CoGe_2$ structure). The occurrence of the $CoGe_2$- and $PdSn_2$-type was first concluded from the cell parameters obtained from a trial-and-error indexing of the powder patterns[10] and confirmed by single-crystal X-ray structure determinations.

X-ray Structure Determination. Suitable single crystals for X-ray structure determination were selected from the samples C. The crystal dimensions for the $CoGe_2$ form were 0.06 × 0.05 × 0.02 mm and those of the $PdSn_2$ form 0.06 × 0.05 × 0.07 mm. For both dimorphs one hemisphere of data were collected at room temperature with Mo Kα radiation (graphite monochromator) on an Enraf-Nonius CAD4 diffractometer with the $\omega-2\theta$ scan type in the range of $2° \le 2\theta \le 70°$ (index limits for the $CoGe_2$ form $-10 \le h \le 10$; $-10 \le k \le 10$; $0 \le l \le 19$ and those of the $PdSn_2$ form $-10 \le h \le 10$; $-10 \le k \le 10$; $0 \le l \le 38$). Some details of the single crystal data collection are listed in Table 1, and in Table 2 the atomic positions and equivalent temperature factors for the dimorphs of $Co_{0.625}Ni_{0.375}Sn_2$ are given.

Table 1. Crystallographic Data for the Dimorphs of $Co_{0.625}Ni_{0.375}Sn_2$

	$Co_{1-x}Ni_xSn_2$ ($CoGe_2$ form)	$Co_{1-x}Ni_xSn_2$ ($PdSn_2$ form)
chem form	$Co_{0.60}Ni_{0.40}Sn_2$	$Co_{0.63}Ni_{0.37}Sn_2$
space group	*Aba*2 (No. 41)	$I4_1/acd$ (No. 142)
lattice constants, Å	$a = 6.2439(4)$	$a = 6.2360(5)$
	$b = 6.2493(4)$	
	$c = 11.778(1)$	$c = 23.588(2)$
volume, Å^3	459.56(6)	917.3(1)
Z	8	16
density (calcd), g/cm^3	8.56	8.58
T, K	295	295
wavelength, Å^{-1}	0.710 69 (Mo Kα)	0.710 69 (Mo Kα)
abs coeff, mm^{-1}	28.24	28.31
$R1^a$ [$\lvert F\rvert^2 > 2\sigma(\lvert F\rvert^2)$]	0.020	0.029
$R_w{}^b$ [$\lvert F\rvert^2 > 2\sigma(\lvert F\rvert^2)$]	0.039	0.062

^{a} $R = [\sum(|F_o| - |F_c|)]/\sum|F_o|$. ^{b} $R_w = \{[\sum w(F_o^2 - F_c^2)^2]/\sum w(F_o^2)^2\}^{1/2}$; $w = [\sigma^2(|F_o|^2 + (aP)^2 + bP]^{-1}$; $P = (F_o^2(\ge 0) + 2F_c^2)/3$. ($a = b = 0$ for the CoGe2 form; $a = 0.0231$ and $b = 17.62$ for the $PdSn_2$ form).

Analytical absorption corrections were applied which improved the quality of the $PdSn_2$ structure intensity data only slightly ($R_{int}(F_o^2) = 5.6/5.5$ (8 unique sets), $R(F)$ for $F_o^2 > 2\sigma(F_o^2) = 3.0/2.9$) but drastically improved that of the $CoGe_2$ data ($R_{int}(F_o^2) = 10.8/4.9$ (4 unique sets), $R(F)$ for $F_o^2 > 2\sigma(F_o^2) = 7.6/2.0$), reflecting the shape of the crystals. The crystal structures were refined using full-matrix least-squares refinement on F^2 (program SHELXL-93[11]) with the scattering factors of Co and Sn. The compositions of the actual crystals were determined by EDX analyses after having collected the X-ray data. The composition of the crystal with the $CoGe_2$ structure ($Co_{0.60}Ni_{0.40}Sn_2$) deviated slightly from the mean composition of sample C ($Co_{0.625}Ni_{0.375}Sn_2$).

In the refinement of the $PdSn_2$ structure the anisotropic displacement parameters U_{11} and U_{22} of Co and Sn2 were highly correlated because these two kinds of atoms lie on or very close to the $\bar{4}$ and the 4_3 axis respectively. Thus, we introduced the constraint $U_{11} = U_{22}$ for these atoms. In the refinement of the $CoGe_2$ structure, the difference Fourier map revealed an electron density maximum at the position ($\sim y_{Sn1}$, $\sim x_{Sn1}$, $\sim z_{Sn1}$). This was suspected to be a consequence of stacking disorder along the c axis and/or the occurrence of microscopic or macroscopic twin domains in the crystal. Attempts to adapt macroscopic twin models could not remove the density maximum. We, therefore, concluded the occurrence of stacking disorder or microscopic domain twinning and refined this density maximum as a Sn1 split position (Sn1′ at ($\sim y_{Sn1}$, $\sim x_{Sn1}$, z_{Sn1})). This improved the R value from 2.9 to 2.0 ($R(F)$ for $F_o^2 > 2\sigma(F_o^2)$) and left the difference Fourier map featureless (largest peak 2.08 e/Å^3, largest hole −1.51 e/Å^3). The thermal displacement parameters of the two Co atoms were highly correlated and, thus, fixed to have the same values. The correlation is due to the fact that in a single building block the two atoms are related by a mirror plane which is not present in the complete structure (cf. Figures 5a and 5b).

DSC Investigations. We performed DSC (differential scanning calorimetry) investigations on the $PdSn_2$ and $CoGe_2$ modification of $Co_{0.625}Ni_{0.375}Sn_2$ (sample C) by heating and cooling the samples at a rate of 10 K/min. We could not detect any thermal effect indicating a phase transition from the $PdSn_2$ form to the $CoGe_2$ form. The $PdSn_2$ form melted at 559 °C and recrystallized in the $CoGe_2$ modification, which was obtained quantitatively after two heating/cooling cycles. The $CoGe_2$ form melted at 556 °C. Even with annealing experiments at temperatures around 500 °C over a period of several weeks, it was not possible to obtain the $PdSn_2$ modification from the $CoGe_2$ form.

TEM Investigations. Samples were ground under ethanol and dispersed on copper grids coated with holey-carbon support film. The TEM studies were carried out in a JEOL 2000FX electron microscope fitted with a double-tilt stage for reciprocal space exploration and low-resolution imaging. High-resolution imaging was performed in a JEOL 4000EX electron microscope (400 kV, Cs = 1.0, structural resolution

(8) Jeitschko, W.; Jaberg, B. *Acta Crystallogr., Sect. B: Struct. Sci.* **1982**, *B38*, 598.
(9) Lang, A.; Jeitschko W. *Z. Metallkd.* **1996**, *87*, 759.
(10) Werner, P.-E. *TREOR Trial-and-error program for indexing of unknown powder patterns*; University of Stockholm: Stockholm, Sweden, 1988.
(11) Sheldrick, G. M. *SHELXL-93 Program for the Refinement of Crystal Structures*; University of Göttingen: Göttingen, FRG, 1993.

Table 2. Atomic Coordinates, Occupancies, and Equivalent Isotropic Displacement Parameters (Å^2) for the Dimorphs of $Co_{0.625}Ni_{0.375}Sn_2$

atom	site	*x*	*y*	*z*	SOF	U_{iso}, 10^4 Å^2
			$CoGe_2$-Type			
T(Co,Ni)1	4a	0	0	0.13507	1	77(1)
T(Co,Ni)2	4a	0	0	0.3650(1)	1	77(1)
Sn1	8b	0.33644(5)	0.16255(5)	0.2513(3)	0.967(2)	76(1)
Sn1′	8b	0.160(2)	0.337(2)	0.2513(3)	0.033(1)	76(1)
Sn2	8b	0.2485(2)	0.25678(5)	0	1	85(1)
			$PdSn_2$-Type			
T(Co,Ni)	8b	0	0.25	0.31765(4)	1	69(2)
Sn1	16f	0.16356(6)	0.41356(6)	0.125	1	72(2)
Sn2	16e	0.24234(8)	0	0.25	1	74(2)

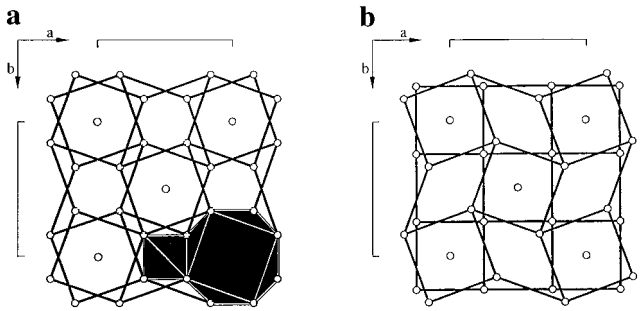

Figure 3. (a) The $CuAl_2$ structure. (b) Arrangement of alternately stacked 3^2434 and 4^4 nets. Circles in the net corners denote E atoms; circles in the center of the squares represent T atoms.

= 1.6 Å). Image simulations were calculated with the NCEMSS program system[12] using multislice algorithms.

Results and Discussion

Structural Relationships. The increase of the Ni content in the system $Co_{1-x}Ni_xSn_2$ induces a phase transition from the $CuAl_2$ structure to either the $CoGe_2$ or the $PdSn_2$ structure. We found for the $CuAl_2$-type a limiting composition $Co_{0.93(2)}Ni_{0.07(2)}Sn_2$ and for $Co_{1-x}Ni_xSn_2$ in the $CoGe_2$ or $PdSn_2$ structure a homogenity range of $0.23(3) < x < 0.59(3)$ for both modifications. This was concluded from EDX analyses of $CuAl_2$-, $CoGe_2$-, and $PdSn_2$-type crystals in samples A and E.

In the $CuAl_2$ structure of $Co_{0.93}Ni_{0.07}Sn_2$ (space group symmetry *I*4/*mcm*), Sn atoms form 3^2434 nets which are stacked exactly on top of each other in an anti-position (staggered) orientation. This leads to a tetragonal assembly of rows of edge-sharing tetrahedra and face-sharing square antiprisms (Figure 3a). All of the antiprisms are occupied by the T atoms. When exchanging every second 3^2434 net for a 4^4 net in the $CuAl_2$ structure, a hypothetical structure is obtained in which the coordination polyhedron for the T atoms is between a cube and a square antiprism (Figure 3b). This structure has space group symmetry *P*4/*mbm* and can serve as an aristotype structure to the $PdSn_2$- and $CoGe_2$-types. In the following we refer to the $CuAl_2$ structure as aristotype-I and the structure containing 4^4 nets as aristotype-P. Further, we call the plane of the nets the (*a*,*b*) plane and the direction perpendicular to it the *c* direction. From the two aristotypes more structures can be derived by applying crystallographic shearing[6] to blocks defined by several consecutive nets. These blocks are simply mutually shifted by the vectors ($^1/_2$,0), (0,$^1/_2$), or ($^1/_2$,$^1/_2$) in the (00*l*) planes. The effect of the shear operations is demonstrated in parts a−d of Figure 4. The shift ($^1/_2$,0) creates an anti-phase boundary with respect to two neighboring 3^2434 nets (Figure 4a), thus intersecting the infinite chains of T atoms. The shift ($^1/_2$,$^1/_2$) transforms an ensemble of two equally oriented 3^2434 nets into

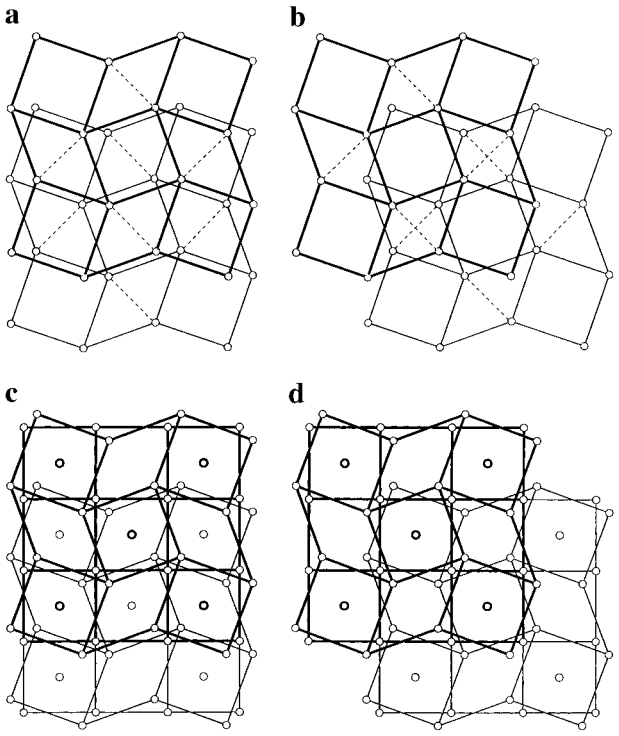

Figure 4. Applications of crystallographic shear operations to a sequence of two 3^2434 nets (a) translation ($^1/_2$,0) and (b) translation ($^1/_2$,$^1/_2$) and a sequence of 3^2434 and 4^4 nets (c) translation ($^1/_2$,0), (d) translation ($^1/_2$,$^1/_2$). The bold nets are situated above the others.

the anti-position orientation and *vice versa* (Figure 4b). Note that the 4^4 nets are invariant under these operations (Figure 4c,d). With the shifts ($^1/_2$,0) and (0,$^1/_2$), the 4-fold axis in the *c* direction disappears and the resulting arrangement has orthorhombic symmetry with *a* and *b* axes of the same length. Applied to two consecutive 3^2434 nets, this shift puts a diamond on top of a square. Apparently this combination does not offer a suitable coordination for the T atoms because in structures TE_n derived from the $CuAl_2$ structure (e.g., the structures of β-$CoSn_3$ and $PdSn_3$) T atoms are removed between two nets arranged in this way.

The structure of $CoGe_2$ follows from the aristotype-P with the ensemble $4^4-3^2434-4^4$ as the building block A (shown in Figure 5a) and the ($^1/_2$,0) shift as the shearing operation (cf. Figure 4c). In the three layer building block the T atoms are located in pairs. For convenience, we chose building blocks for structures derived from this aristotype structure to be bounded by 4^4 nets. The total structures result when the mutually shifted building units are *condensed* in the *c* direction, thus sharing the bounding 4^4 nets. In the orthorhombic structure of $CoGe_2$ the stacking sequence is $A_{(0,0)}B_{(1/2,0)}$, where the shift vector relative to A is specified in subscripts. T atoms are situated between all nets (Figure 5b). In the $PdSn_2$ structure, the same building unit is used but the sequence

(12) Kilaas, R. *45th Annual Proceedings of the Electron Microscopy Society of America*, Baltimore, Maryland, 1987; p 66.

Table 3. Selected Bond Distances (Å) in the Dimorphs of $Co_{0.625}Ni_{0.375}Sn_2$[a]

			$CoGe_2$-Type				
T1−Sn2	2.703(1) [2]	T2−Sn1	2.690(2) [2]	Sn1−T2	2.690(2)	Sn2−T2	2.692(1)
T1−Sn1	2.705(2) [2]	T2−Sn2	2.692(2) [2]	Sn1−T2	2.699(2)	Sn2−T1	2.703(1)
T1−T2	2.708(2)	T2−Sn1	2.699(2) [2]	Sn1−T1	2.705(2)	Sn2−T1	2.741(1)
T1−Sn1	2.714(2) [2]	T2−T1	2.708(1)	Sn1−T1	2.714(2)	Sn2−T2	2.751(1)
T1−Sn2	2.741(1)	T2−Sn2	2.751(1) [2]	Sn1−Sn1	2.881(1)	Sn2−Sn1	3.035(3)
				Sn1−Sn2	3.035(3)	Sn2−Sn1	3.067(3)
				Sn1−Sn2	3.067(3)	Sn2−Sn2	3.123(1) [2]
				Sn1−Sn1	3.306(1) [2]	Sn2−Sn2	3.125(1) [2]
				Sn1−Sn1	3.308(1) [2]		
			$PdSn_2$-Type				
		T−Sn2	2.695(1) [2]	Sn1−T	2.697(1) [4]	Sn2−T	2.695(1) [2]
		T−Sn1	2.697(1) [4]	Sn1−Sn1	2.885(1)	Sn2−T	2.749(1) [2]
		T−T	2.706(2)	Sn1−Sn2	3.054(1) [2]	Sn2−Sn1	3.054(1) [2]
		T−Sn2	2.749(1) [2]	Sn1−Sn1	3.299(1) [4]	Sn2−Sn2	3.118(1) [2]
						Sn2−Sn2	3.120(1) [2]

[a] The numbers in square brackets indicate the frequencies.

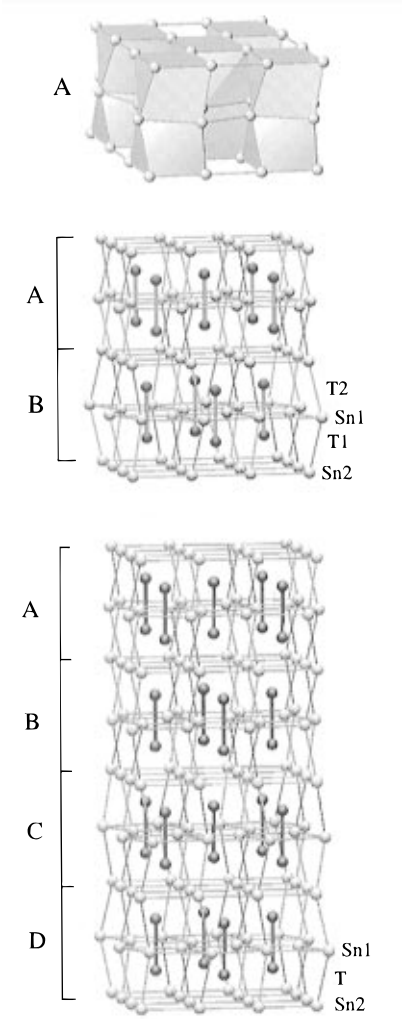

Figure 5. (a) Building block A of the $CoGe_2$ and the $PdSn_2$ structure type. (b) AB stacking sequence in the $CoGe_2$ structure of $Co_xNi_{1-x}Sn_2$. (c) ABCD stacking sequence in the $PdSn_2$ structure of $Co_xNi_{1-x}Sn_2$. The pairs of T atoms are represented as joined dark circles.

$A_{(0,0)}B_{(1/2,0)}C_{(1/2,1/2)}D_{(0,1/2)}$ is realized, doubling the translational period compared to the $CoGe_2$ structure. In addition, this sequence introduces $\bar{4}$, 4_1, and 4_3 axes in the *c* direction, thus leading to tetragonal symmetry for $PdSn_2$ (Figure 5c). The first coordination sphere of the atoms is not affected by the different stacking sequences, and in $Co_{0.625}Ni_{0.375}Sn_2$ the interatomic distances in the building blocks of the two crystal structures are virtually identical (Table 3). Besides $Co_{1-x}Ni_xSn_2$ and $CoGe_2$,[13] which was reported with the compostion $Co_{0.9}Ge_2$, only the ternary compound Ni_2GaGe_3[14] is known to adopt the $CoGe_2$ structure.[15] The earlier reported modifications of $PdSn_2$ and $RhSn_2$ with this structure type[13] could not be reproduced by Hellner.[16] In the investigated $CoGe_2$-type crystals of $Co_{1-x}Ni_xSn_2$, we could not detect any significant deviation from full occupancy for the T positions. The known representatives of the $PdSn_2$ structure type include, apart from $PdSn_2$ and $Co_{1-x}Ni_xSn_2$, the compounds Ni_3ZnGe_5 and $Pd_3Sb_2In_4$.[15] Of the latter only lattice constants obtained from X-ray powder diagrams are reported,[17] whereas for $PdSn_2$ atomic parameters from a single-crystal investigation exist.[16] The structure of $RhSn_2$ is the third known representative of this family of structures derived from aristotype-P by applying the above-mentioned shear operations. In $RhSn_2$, a five-layer building block is stacked with the $A_{(0,0)}B_{(1/2,0)}$ sequence.[16]

Examples derived from aristotype-I ($CuAl_2$ structure) are the structures $PdSn_3$[18] and β-$CoSn_3$.[9] $PdSn_3$ is obtained by applying the ($^1/_2$,0) shear operations to three-layer blocks (corresponding to the translational period of $CuAl_2$) and removing the T atoms between shifted layers because of their unfavorable coordination (cf. Figure 4a). This changes the composition from TE_2 to TE_3. In the orthorhombic $PdSn_3$ structure, the stacking sequence of the three-layer blocks containing pairs of T atoms is $A_{(0,0)}B_{(1/2,0)}$. In the recently reported structure of β-$CoSn_3$, these three-layer blocks of the $CuAl_2$ structure are stacked in an $A_{(0,0)}B_{(1/2,0)}C_{(1/2,1/2)}D_{(0,1/2)}$ sequence, and thus $PdSn_3$ and $CoSn_3$ are related in the same way as is the pair $CoGe_2$/$PdSn_2$. Interestingly, the compound $CoSn_3$ shows the same kind of dimorphism with α-$CoSn_3$ adopting the $PdSn_3$ structure.[9]

We conclude that starting from a set of tetragonal aristotype structures, where 3^2434 nets or alternately 3^2434 and 4^4 nets are stacked on top of each other, crystallographic shearing explains two classes of related observed structures: orthorhombic (pseudotetragonal) structures are obtained when mutually

(13) Schubert, K.; Pfisterer, H. *Z. Metallkd.* **1950**, *41*, 433.
(14) Panday, P. K.; Schubert, K. *J. Less-Common Met.* **1969**, *18*, 175.
(15) Villars, P.; Calvert, L. D. *Pearsons Handbook of Crystallographic Data for Intermetallic Compounds*, 2nd ed.; ASM International: Materials Park, OH, 1991.
(16) Hellner, E. *Z. Kristallogr.* **1956**, *107*, 99. The position of the Pd atoms in $PdSn_2$ was given as (0, $^1/_4$, 0.467). This is far from the idealized position (0, $^1/_4$, 0.3125) situated exactly between a 3^2434 and a 4^4 net formed by Sn atoms, which is almost realized in $Co_{1-x}Ni_xSn_2$ (T atom position (0, $^1/_4$, 0.31765)). We prepared samples of $PdSn_2$ and compared the powder patterns with theoretical calculated ones using different *z* values for the Pd position (program LAZY-PULVERIX, Yvon, K.; Jeitschko, W; Parthé, E. *J. Appl. Crystallogr.* **1977**, *10*, 73). We only found agreement when Pd atoms are situated close to the idealized position between the nets, in accordance with the compound $Co_{1-x}Ni_xSn_2$.
(17) El-Boragy, M.; Schubert, K. *Z. Metallkd.* **1971**, *62*, 667.
(18) Schubert, K.; Lukas, H. L.; Meissner, H.-G.; Bhan, S. *Z. Metallkd.* **1959**, *50*, 534.

Table 4. *d*-Spacings of the Idealized Structures of $CoGe_2$ and $PdSn_2$

d (Å)	*hkl* $CoGe_2$ (AB)	*hkl* $PdSn_2$ (ABCD)	*d* (Å)	*hkl* $CoGe_2$ (AB)	*hkl* $PdSn_2$ (ABCD)
5.875	0,0,2	0,0,4	1.7659	2,2,4	2,2,8
4.1365	1,1,1	1,1,2	1.7645	3,1,3; 1,3,3	3,1,6
3.1250	2,0,0; 0,2,0	2,0,0	1.7334	3,2,0	
3.0200		2,0,2	1.7287		3,2,1
2.9375	0,0,4	0,0,8	1.7149	2,3,1	
2.9312	1,1,3	1,1,6	1.6973		2,1,11
2.7951	1,2,0		1.6925		3,2,3
2.7755		2,1,1	1.6626	3,2,2	
2.7590	2,0,2; 0,2,2	2,0,4	1.6594	2,0,6; 0,2,6	2,0,12
2.7192	2,1,1		1.6398		3,1,8
2.6325		2,1,3	1.6264		3,2,5
2.5240	1,2,2		1.6039	1,2,6	
2.4427		2,0,6	1.5851	2,3,3	
2.4024		2,1,5	1.5692	1,1,7	1,1,14
2.2752	2,1,3		1.5625	4,0,0; 0,4,0	4,0,0
2.2097	2,2,0	2,2,0	1.5489		4,0,2
2.1480		2,1,7	1.5402		3,2,7
2.1403	2,0,4; 0,2,4	2,0,8	1.5179		2,1,13
2.0749	1,1,5	1,1,10	1.5158	1,4,0	
2.0683	2,2,2	2,2,4	1.5127		4,1,1
2.0249	1,2,4		1.5126	1,3,5; 3,1,5	3,1,10
1.9583	0,0,6	0,0,12	1.5100	0,4,2; 4,0,2	4,0,4
1.9490	1,3,1; 3,1,1	3,1,2	1.5034	4,1,1	
1.9081		2,1,9	1.4929	3,2,4	
1.8782		2,0,10	1.4882		4,1,3
1.8733		3,1,4	1.4787		2,0,14
1.7987	2,1,5		1.4688	0,0,8	0,0,16

shifted building blocks are stacked in an AB sequence, tetragonal structures result from an ABCD sequence of the building blocks. Importantly, consecutive building blocks are always shifted by either the vector ($^1/_2$,0) or (0,$^1/_2$) thus avoiding a linear chain arrangement of the T atoms.

Dimorphism of $Co_{1-x}Ni_xSn_2$ ($0.23 < x < 0.59$). The melting point and melting enthalpy of the $PdSn_2$ form of $Co_{1-x}Ni_xSn_2$ is slightly but significantly higher than that of the $CoGe_2$ modification. Therefore, we assume the $PdSn_2$ structure to be the ground-state or low-temperature modification in the system $Co_{1-x}Ni_xSn_2$ ($0.23 < x < 0.59$).[19] Note that in our experiments we could not obtain the ABCD-stacked $PdSn_2$ modification using the AB-stacked $CoGe_2$ modification as the starting material. Apparently the ABCD stacking sequence forms only in the presence of a flux at synthesis temperatures of 500 °C and below. Increasing the flux temperature to 550 °C leads to the formation of the AB sequence of the $CoGe_2$ modification, but Guinier powder patterns still reveal weak lines belonging to the $PdSn_2$-type. The question arises if the product of flux synthesis at a temperature between 500 and 550 °C represents a mixture of ABCD- and AB-stacked crystals or if the particular crystals consist of intergrowths of both types of stacking sequences. This would even include the possibiltiy of new stacking sequences.

Stacking Disorder. A first indication of the occurrence of stacking disorder was the detection of a split position for the 3^2434-forming Sn atoms (Sn1) atoms at ($\sim y_{Sn1}$, $\sim x_{Sn1}$, z_{Sn1}) in the refinement of $Co_{1-x}Ni_xSn_2$ in the $CoGe_2$ structure. This corresponds to the anti-position orientation of the 3^2434 net. If only using the shifts ($^1/_2$,0) and (0,$^1/_2$) between adjacent building blocks, stacking disorder can be introduced by exchanging some of the A(B)-oriented building blocks by C(D) oriented ones. Thus, small areas "...ABAB..." of a $CoGe_2$-type crystal might be transformed into a domain "...ABCB...", or "...ABAD...", or even "...ABCD..." (one unit cell $PdSn_2$). In such domains, 3^2434 nets are partly oriented in an anti-position. Allowing, additionally, the shift ($^1/_2$,$^1/_2$), the staggered orientation is directly obtained in two consecutive building blocks AC (BD). From the refined site occupancy, we conclude that in the $CoGe_2$-type crystal with the data presented in Table 2 3.3(1)% of the building blocks are stacked in a C or D orientation. In another crystal

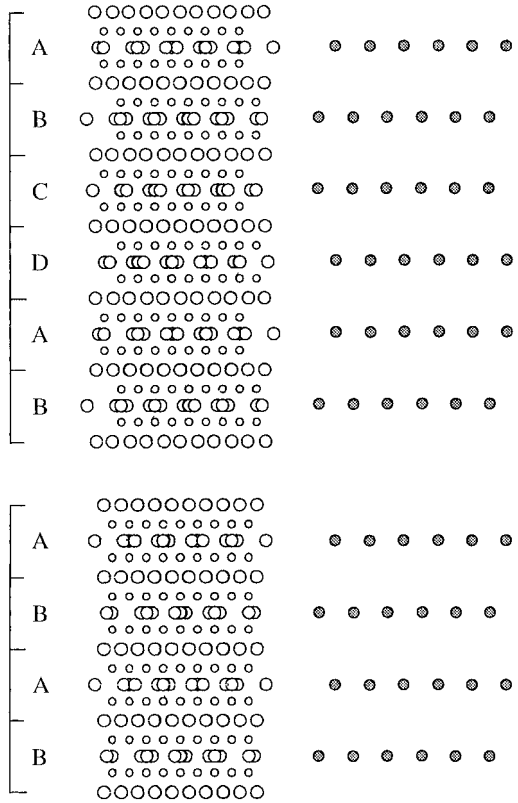

Figure 6. [1$\bar{2}$0] projection of (a) the $PdSn_2$ structure and (b) the $CoGe_2$ structure. The large circles are Sn atoms, and the small circles are T atoms. The building blocks and their stacking sequence are marked in the left-hand part of the figure. In this projection, only 3^2434 net-forming Sn atoms can be resolved in electron microscope high-resolution images ($d_{Sn-Sn} > 1.6$ Å). In the right-hand part, the average positions of the 3^2434 net-forming Sn atoms in the [1$\bar{2}$0] projection are drawn.

(19) For the compound $CoSn_3$, Lang and Jeitschko[9] found the modification with the lower symmetric $PdSn_3$ structure as the low-temperature form.

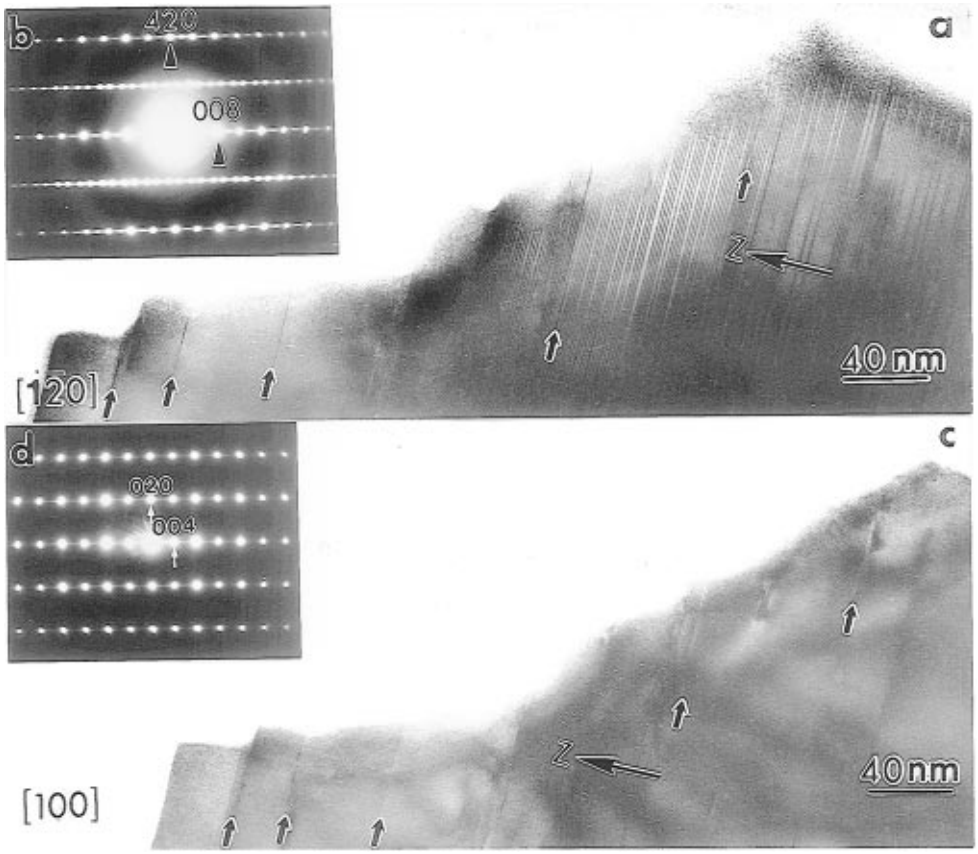

Figure 7. Low-resolution micrographs from the same crystal $Co_xNi_{1-x}Sn_2$ ($0.23 < x < 0.59$) oriented along (a) [1$\bar{2}$0] and (c) [100]. Inset (b, d) are the corresponding selected area diffraction (SAED) patterns. Building block faults are marked in both micrographs with small black and white arrows. The *c* direction is indicated by the big arrow.

with the same composition, we found this value to be 5.4(1)%. Lang and Jeitschko also noticed this kind of split position for $CoSn_3$ in the AB-stacked $PdSn_3$ structure (5.2(9)% site occupancy).[9] For $RhSn_2$, which consists like $CoGe_2$ and $PdSn_2$ of alternately-stacked 3^2434 and 4^4 nets, single-crystal X-ray diffraction photographs revealed tetragonal symmetry and the occurrence of rows of diffuse reflection spots with the condition *hkl*: $h + k = 2n + 1$.[16] This was interpreted as the result of a stacking sequence (A,C)(B,D) where A/C- and B/D-oriented blocks with the same frequency and probability emulate tetragonal symmetry.

Apart from the stacking disorder of building blocks, we have to consider a second kind of disorder which affects the building unit itself. In the case of the structures $PdSn_2$ and $CoGe_2$, one can imagine that a single building block might be destroyed by a sequence of two consecutive 3^2434 or 4^4 nets. In the following, we call this kind of defect building block fault. When comparing the *d*-spacings of the (idealized) $CoGe_2$ and the $PdSn_2$ structure (Table 4), it becomes clear that only reflections with *hkl*: $h + k = 2n + 1$ in the reciprocal planes {2*hhl*} express the difference between an ABAB- and an ABCD-stacked structure. The real space correspondence is shown in Figure 6, where the $PdSn_2$ and the $CoGe_2$ structure are drawn in one of the $\langle 1\bar{2}0 \rangle$ projections. It is seen that it is indeed possible to distinguish if a building block is either A/D or B/C arranged. On the contrary, in the [110] projection A- and C-arranged blocks appear to be the same, as well as B- and D-arranged ones, and this makes the ABCD sequence ($PdSn_2$) undistinguishable from the ABAB sequence ($CoGe_2$). In the [100] projection, none of the blocks A, B, C, D can be distinguished and all possible stacking variants look like the simple AA sequence of the aristotype-P structure. This means that the reciprocal lattice planes (0*kl*) and (*h*0*l*) are invariant to changes in the stacking sequence but on the other hand should reveal the presence of building block disorder. Consequently, the investigation on stacking and building block disorder can be confined to a study of the reciprocal planes (2*hhl*) and (0*kl*), and the method of choice for such studies is selected area electron diffraction (SAED).

Microscopic Analysis of the Stacking Disorder. Figure 7 shows nicely the complementary information in the reciprocal (2*hhl*) and (0*kl*) planes or alternatively the [1$\bar{2}$0] and [100] projections. In Figure 7a the crystal is oriented along [1$\bar{2}$0], and especially on the right-hand part of the figure an accumulation of stacking disorder is discernible. Note that only building block faults are marked with arrows. In the corresponding SAED pattern (Figure 7b), stacking disorder is noticeable as diffuse intensity streaks with an additional intensity modulation in the reflection rows 21*l* and $\bar{2}1l$. The diffuse intensity observed in the rows 00*l*, 42*l*, and $\bar{4}2l$ is not due to the stacking disorder but is caused by double diffraction phenomena.[20] When the same crystal is oriented along [100] (Figure 7c), the stacking disorder becomes invisible but the building block defects marked with arrows remain. In the corresponding SAED pattern (Figure 7d), these building block faults are indicated by the weak diffuse streaking in the *c** direction, which affects all rows of reflections. Note that this weak diffuse-streaked intensity cannot be a obtained from the reflection rows *hkl*: $h + k = 2n + 1$ by double diffraction because they are absent in the reciprocal plane (0*kl*).

(20) Double diffraction consists in the redistribution of diffracted intensity in a diffraction pattern by the scattering of an already diffracted electron along any other allowed diffraction path. Consequently, any electron from the diffuse-streaked 21*l* row, for example, can diffract a second time with the crystal along the $\bar{2}10$ diffraction path to add intensity to the 00*l* reflection row in the final pattern.

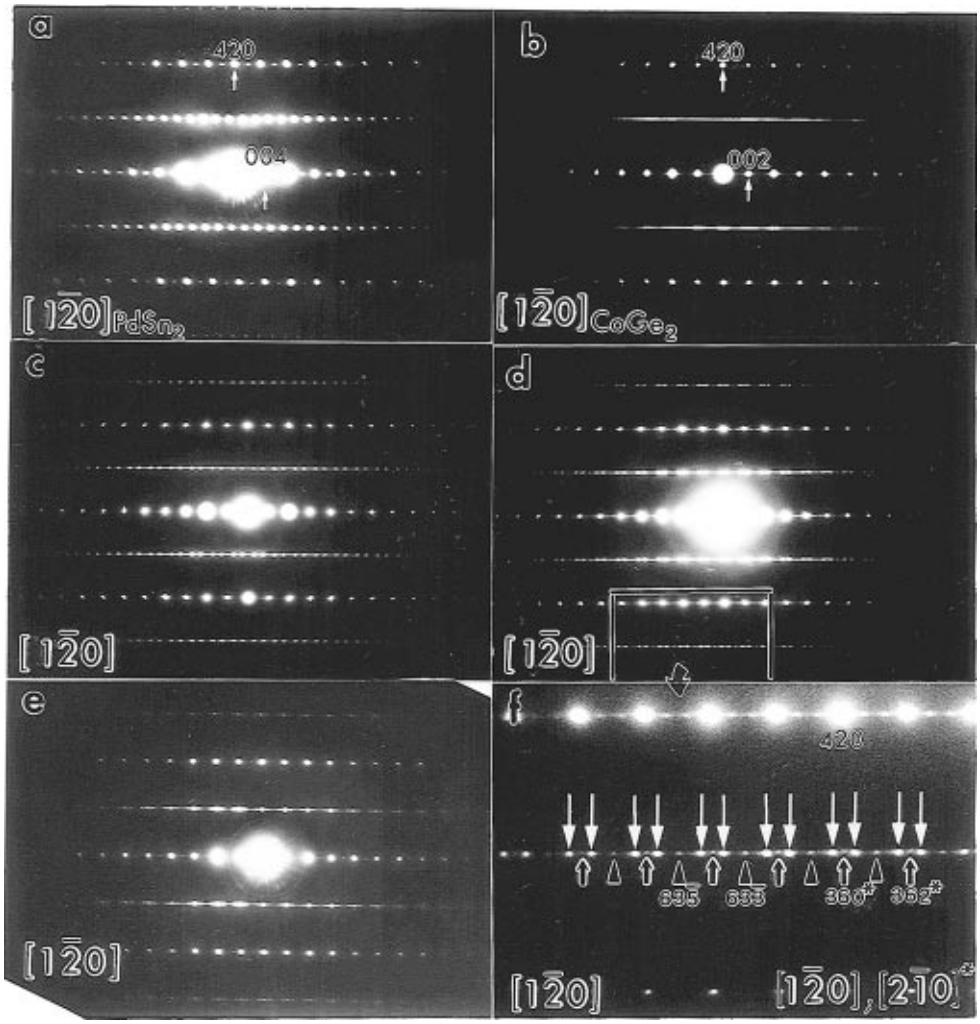

Figure 8. SAED patterns from different crystals of $Co_xNi_{1-x}Sn_2$ along their [1$\bar{2}$0] zone axes. (a) SAED pattern from a crystal with the $PdSn_2$ structure type. The forbidden reflections 002, 006, ... appear by double diffraction[20] from the 21*l* reflections. (b) SAED pattern of a randomly disordered crystal. The reflection indices refer to the $CoGe_2$ structure type. (c−e) SAED patterns of different crystals exhibiting different degrees of disorder: (c,d) predominance of the ABCD stacking sequence, (e) predominance of the AB stacking sequence. (f) Amplification of the area marked in (d). The zone axis in the down-left corner refers to the $PdSn_2$ structure, while the zone axes in the down-right corner refer to the $CoGe_2$ structure. White arrows indicate reflections from the incommensurate, basically ABCD-stacked domain, black and white arrowheads indicate reflections from the $CoGe_2$ domain in the [1$\bar{2}$0] orientation (AB sequence, indices without asterisk), and black and white arrows indicate reflections originated from the $CoGe_2$ domain in the [$\bar{2}$10]) orientation (AD sequence, indices with asterisk).[21]

Most of the crystals of the $PdSn_2$ modification studied by electron diffraction exhibited a perfectly ordered ABCD stacking sequence (Figure 8a), while we have not found any crystal in a perfect AB-stacked $CoGe_2$ structure. As expected, a variety of different kinds of stacking disorder could be detected in the samples of flux syntheses performed at 550 °C, and in the following some examples are presented. In the diffraction pattern of Figure 8b, the rows of relections with *hkl*: $h + k = 2n + 1$ are completely diffuse, which means that A- and B-oriented blocks in the AB sequence of the $CoGe_2$ structure are randomly exchanged by C- and D-oriented ones, respectively. This corresponds exactly to the stacking situation of the above-mentioned $RhSn_2$ structure with a sequence (A,C)-(B,D). Apart from the case of random disorder, the homogenous introduction of stacking faults may give rise to statistically new unit cells. These unit cells can be incommensurate with the basic unit cell. In Figure 8c,d, the ABCD stacking sequence dominates in the diffraction patterns. In the perfectly ordered $PdSn_2$ structure the periodicity is $2 \times (002)$ (Figure 8a), whereas we estimated a periodicity of $\sim 2.43 \times (002)$ in Figure 8c and of $\sim 2.95 \times (002)$ in Figure 8d. In Figure 8e, the AB sequence dominates in the diffraction pattern and the introduction of stacking faults resulted in a new commensurate periodicity of $\sim 7 \times (002)$. Figure 8f is an amplification of the the area marked in Figure 8d and reveals that this diffraction pattern is actually composed of several parts.[21]

Figure 9 shows a micrograph from a crystal where domains of AB ($CoGe_2$), AD (twin orientation of $CoGe_2$), and ABCD ($PdSn_2$) are distributed in a disordered way. The electron diffraction inset reveals that the AD-stacked domains are more abundant in the diffracted area of the crystal than are the AB-oriented ones. The black and white line that crosses the image joining white dots emphasizes that the crystal is basically

(21) The diffraction pattern shown in Figure 8f consists of three different parts. There is, first, the pattern of the dominating, basically ABCD-stacked, domain with the almost commensurate periodicity of $2.95 \times (002)$. The reflections of this domain are marked with white arrows. In between we can observe reflections that belong to a domain of AB-stacked building blocks ($CoGe_2$ structure). The third kind of reflections stem from a domain of AD-stacked building blocks, which corresponds to the [$\bar{2}$10] (twin) orientation of the $CoGe_2$ structure. The reflections 63*l* ([120] orientation) appear at slightly smaller d-spacings (bigger reciprocal distances from the transmitted beam) than the reflections 36*l* ([$\bar{2}$10] orientation) due to the small difference in the *a* and *b* lattice constants. The A-centering in the $CoGe_2$ structure forbids the 36*l*: $l = 2n + 1$ and the 63*l*: $l = 2n$ reflections because of the general condition *hkl*: $k + l = 2n + 1$. Reflections forbidden by centering cannot appear by double diffraction.

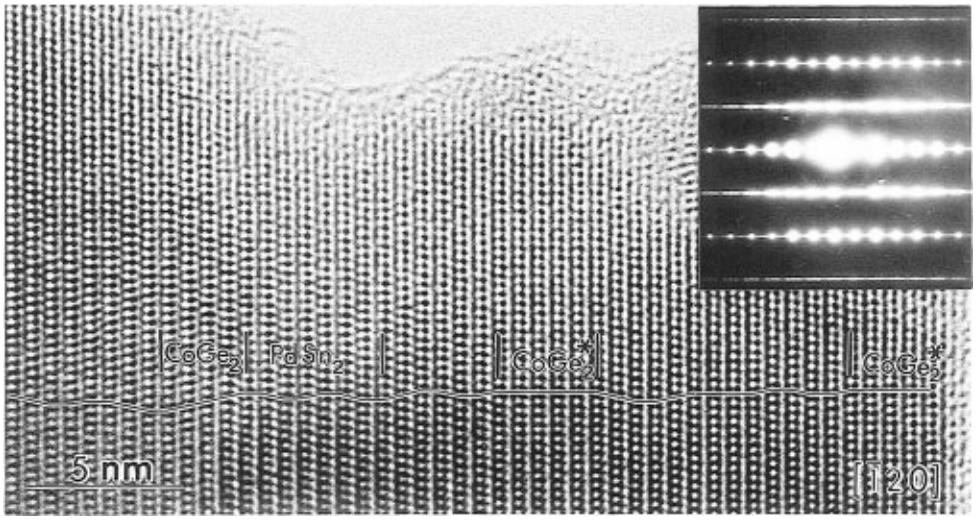

Figure 9. High-resolution micrograph of a crystal of $Co_xNi_{1-x}Sn_2$ ($0.23 < x < 0.59$). Inset is the corresponding SAED pattern. The black and white line running across the image shows the stacking disorder. Areas with ordered $CoGe_2$ and $PdSn_2$ sequences are marked. The asterisk in the label $CoGe_2$* indicates that $CoGe_2$ is oriented along [210] (AD stacking sequence).

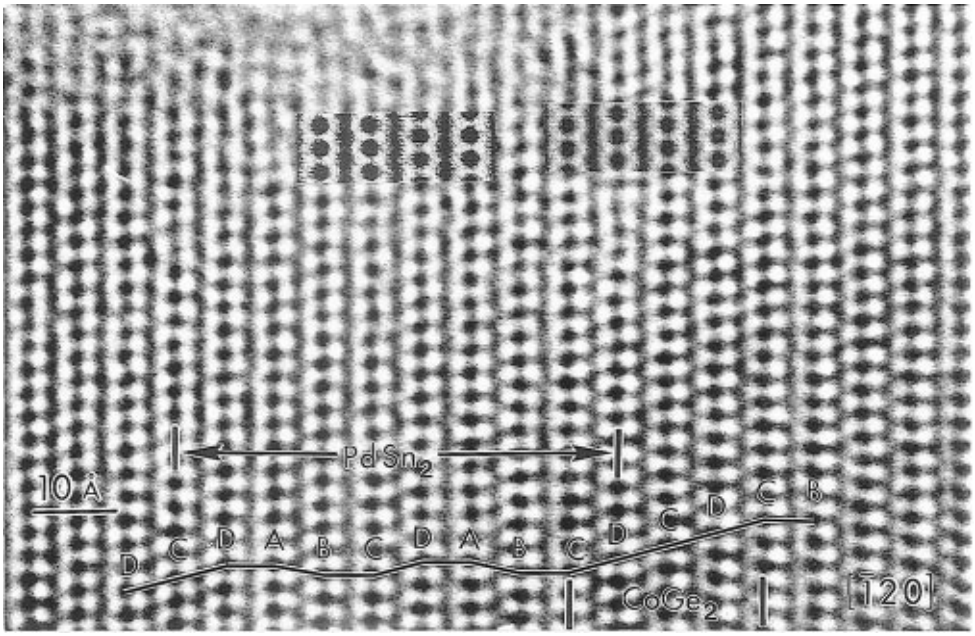

Figure 10. Amplification of a small area of the crystal shown in Figure 9. The white and black line and lettering refers to the stacking sequence of building blocks in a two-unit-cell domain of the $PdSn_2$-type (ABCD) and a two-unit-cell domain of the $CoGe_2$-type (AB = CD). The corresponding simulated images (defocus = −350 Å, thickness = 50 Å) are inset in the upper part of the micrograph.

disordered. Figure 10 represents a high-resolution image of the same crystal shown in Figure 9 with two unit cells of the $PdSn_2$ structure contiguous to two unit cells of the $CoGe_2$ structure, both oriented along [1$\bar{2}$0]. The images calculated by multislice methods[12] for both types of unit cells are inset in the upper part of the figure. As a result of the image calculations, we can assign the black dots in the micrograph to the Sn atoms forming the 3^2434 nets. In the [1$\bar{2}$0] projection, only these atoms are resolved ($d_{Sn-Sn} > 1.6$ Å) and the drawings of the structures in Figure 6 are easily recognized in the micrograph. Figure 11 is taken from a different area of the same crystal in the same orientation and depicts three unit cells of the $CoGe_2$ structure with the AD-stacked ("twin orientation") sequence. Again, the matching of the corresponding calculated image inset in the upper part of the figure is excellent. It is important to note that the [1$\bar{2}$0] projection of an AD-stacked and AA-stacked sequence look the same and that we actually cannot exclude the occurrence of such AA-stacked, aristotype-P-like domains. However, remembering the above discussed building principle of the structures $CoGe_2$ and $PdSn_2$, we consider the formation of such AA (or AC) stacked domains as unlikely. Summarizing the results of the microscopic investigations one can distinguish between three kinds of disorder in the system $Co_{1-x}Ni_xSn_2$ ($0.23 < x < 0.59$): (1) building block faults where the sequence of the single planar nets is changed, (2) intergrowth of domains with the $PdSn_2$ and the $CoGe_2$ structure, and (3) stacking sequences leading to new periodicities, including incommensurate ones.

Concluding Remarks

When increasing the Ni content in the quasibinary system $Co_{1-x}Ni_xSn_2$ from $x = 0.09$ to $x = 0.23$, we observed the structural phase transition $CuAl_2 \rightarrow CoGe_2/PdSn_2$. This transition is assumed to be induced by the change of the VEC from 17.09 to 17.23 electrons per formula unit. The most conspicuous difference between the $CuAl_2$ and the $CoGe_2/PdSn_2$ structure is the arrangement of the T atoms. In the $CuAl_2$ structure the T atoms form linear chains, whereas in the $CoGe_2$ and $PdSn_2$

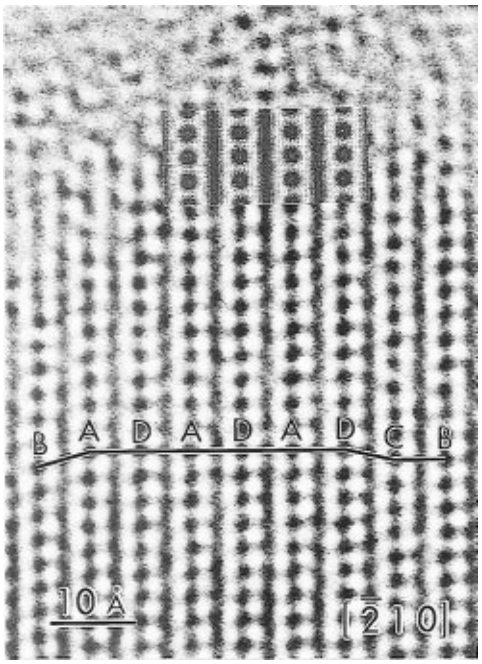

Figure 11. Amplification of a small area of the crystal shown in Figure 9 in the same orientation with a small domain of the $CoGe_2$ structure (three unit cells) along the [$\bar{2}$10] direction. The calculated high-resolution image (defocus = −350 Å, thickness = 50 Å) is inset in the upper part of the micrograph.

structure they are arranged in pairs. Importantly, the introduction of 4^4 nets into the sequence of 3^2434 nets allows the T_2 pair formation without a change of composition. In both kinds of structures, the TSn_8 coordination is very similar. Topologically the breakage of the chains is reminiscent of a Peierls distortion, although the T−T distance changes only slightly from 2.73 Å in $CoSn_2$ to 2.71 Å in $Co_{0.625}Ni_{0.375}Sn_2$.

It is not yet investigated if one-dimensional T−T bonding plays a crucial role in the stability of the $CuAl_2$ structure in systems TE_2, but when inspecting the 18 representatives,[15] it appears that these compounds preferably adopt the $CuAl_2$-type when the VEC is between 15 and 17 electrons per formula unit (cf. Figure 1). The increase of the VEC above the maximum value of 17 could correspond to a situation where strongly T−T antibonding electronic states get occupied, thus supporting a structural phase transition. In systems TE_2 with T being a 4d transition metal, the compound $RhSn_2$ is a representative with a VEC at the phase-transition border. Indeed, $RhSn_2$ is dimorphic and the high-temperature modification crystallizes in the $CuAl_2$ structure. The infinite linear chains of Rh atoms present in this structure type break into three-membered pieces when $RhSn_2$ undergoes the phase transformation to the earlier decribed (randomly disordered) low-temperature modification.

In compounds with the structures $CoGe_2$, $PdSn_2$, or $RhSn_2$, the propensity for stacking disorder is high and we experienced that a combination of X-ray and electron diffraction together with high-resolution microscopy is invaluable for the detailed structural characterization of such systems. As a continuation of this work, we plan a comprehensive analysis of the chemical bonding in the structures of $CuAl_2$ and $CoGe_2/PdSn_2/RhSn_2$ in order to confirm and understand the role of the VEC in the structural phase transitions. Further, it appears to be necessary to explore the influence of the synthesis conditions, especially the temperature, more in detail. It might then be possible to direct syntheses to an exclusive formation of new stacking sequences. Focussing on commensurate periodicities, the number of distinct stacking sequences is rather limited for the simplest cases. When excluding the shifts (0,0) and ($^1/_2$,$^1/_2$) between adjacent building blocks (and thus excluding a chain formation of T atoms), a commensurate periodicity can only be obtained with an even number of building blocks. The first member of this series is the two-block sequence AB (or equivalently AD). With four blocks as the translational period, the sequences ABCD and ABAD are distinct, and with a six-block sequence we find the three possibilities ABCDAB, ABADAB, and ABCBAD.

Acknowledgment. We are grateful to Kjell Jansson, Stockholm University, for performing the DSC measurements. This work was supported by the Swedish National Science Research Council (NFR). U.H. acknowledges a Feodor-Lynen Fellowship of the A. v. Humboldt Foundation.

Supporting Information Available: Tables of the anisotropic thermal parameters for $(Co,Ni)Sn_2$ in the $CoGe_2$ and the $PdSn_2$ structures crystallographic data (2 pages). Ordering information is given on any current masthead page.

IC9703134